VIP Femtochemistry Very Important Paper

Deutsche Ausgabe: DOI: 10.1002/ange.201602523
Internationale Ausgabe: DOI: 10.1002/anie.201602523

The Hydrated Excess Proton in the Zundel Cation $H_5O_2^+$: The Role of Ultrafast Solvent Fluctuations

Fabian Dahms, Rene Costard, Ehud Pines, Benjamin P. Fingerhut, Erik T. J. Nibbering, and Thomas Elsaesser**

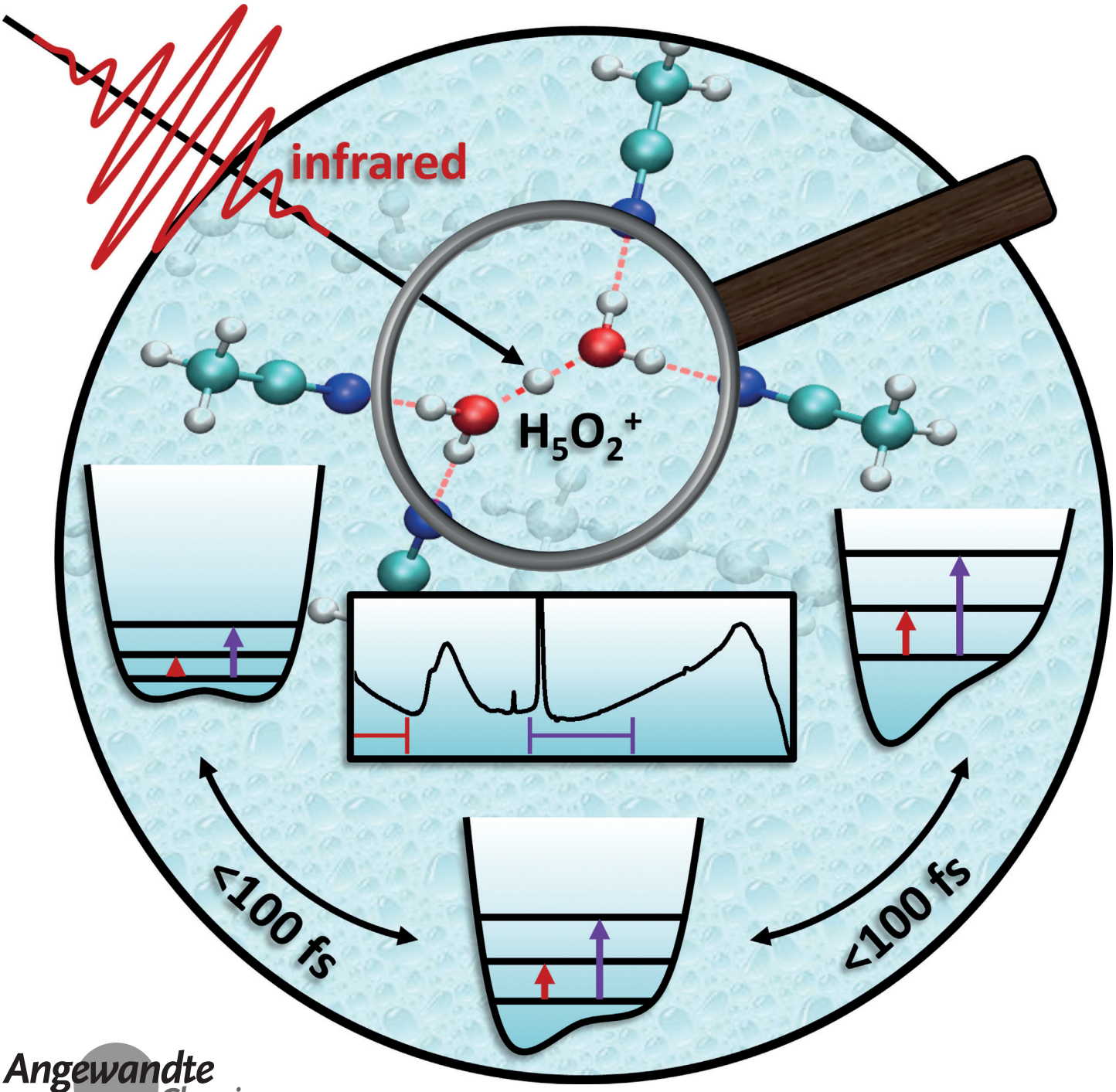

Abstract: *The nature of the excess proton in liquid water has remained elusive after decades of extensive research. In view of ultrafast structural fluctuations of bulk water scrambling the structural motifs of excess protons in water, we selectively probe prototypical protonated water solvates in acetonitrile on the femtosecond time scale. Focusing on the Zundel cation $H_5O_2^+$ prepared in room-temperature acetonitrile, we unravel the distinct character of its vibrational absorption continuum and separate it from OH stretching and bending excitations in transient pump-probe spectra. The infrared absorption continuum originates from a strong ultrafast frequency modulation of the H^+ transfer vibration and its combination and overtones. Vibrational lifetimes of $H_5O_2^+$ are found to be in the sub-100 fs range, much shorter than those of unprotonated water. Theoretical results support a picture of proton hydration where fluctuating electrical interactions with the solvent and stochastic thermal excitations of low-frequency modes continuously modify the proton binding site while affecting its motions.*

The excess proton H^+ plays a central role for fundamental chemical and biochemical processes occurring in both homogeneous and inhomogeneous aqueous environments, such as proton transport in bulk water,[1] hydrogen-fuel cells,[2] acid–base reactions,[3] and proton pumping through membrane proteins.[4] The latter is an archetypical example for processes occurring in biological environments, where the proton is solvated and transferred in partially aqueous environments that are much less polar than bulk water. Amongst such environments are reactive sites of enzymes, proton channels and the surface area of proteins. These biological environments are poorly represented by model systems in bulk water. Solvent systems composed of small amounts of water dissolved in polar aprotic solvents of mild basicity, such as dioxane or acetonitrile, represent an appealing alternative.

In the gas phase two distinctive structures of the hydrated excess proton, the Zundel and the Eigen cation, have been identified by spectroscopy of water clusters.[5] The Zundel cation $H_5O_2^+$[6] consists of two water molecules linked by a strong hydrogen bond through the central H^+ (Figure 1a).[7] The O···O distance of approximately 0.24 nm is substantially smaller than the hydrogen bond length of 0.28 nm in bulk liquid water.[8] The Eigen cation $H_9O_4^+$,[9] that is, $H_3O^+(H_2O)_3$ consists of a central hydronium H_3O^+ forming three equivalent hydrogen bonds of a length of 0.28 nm with the nearest neighbor water molecules. In liquid water, both species are expected to interconvert through intermolecular proton transfer on a time scale shorter than a few picoseconds. According to ab initio or empirical valence bond molecular dynamics calculations, this complex solvation interconversion plays a key role for proton hopping between neighboring water molecules, the well-known von Grotthuss mechanism.[1,10]

The dynamical structural heterogeneity of the excess protons on ultrafast time scales represents a major experimental and theoretical challenge.[10–13] Femtosecond infrared spectroscopy has the potential to map the fluctuating solvation patterns of the hydrated protons in real-time, requiring a link of vibrational bands with specific structural features. However, the most prominent spectroscopic hallmark of solution-phase excess protons, the broad and unstructured infrared absorption bands ("continua")[14] between 1000 and 3000 cm^{-1}, has remained controversial and their origin unclear.

To overcome such problems, we study liquid solutions in which the Zundel cation represents the by far dominating species[15] and apply femtosecond two-color pump-probe spectroscopy in the spectral range from 1500 to 4000 cm^{-1} to discern different contributions to the vibrational response. Below we use the term "Zundel cation" to describe the solvated $H_5O_2^+$ grouping. Zundel cations were prepared in a 0.26 M $HClO_4$/ 0.88 M H_2O solution in acetonitrile (CD_3CN).[15] Acetonitrile was chosen as the medium for the protonated water solvates because of its high polarity and its ability to mix in any proportion with water. Neat acetonitrile is polar enough to support partial ionic dissociation of strong electrolytes and strong mineral acids such as $HClO_4$ and CF_3SO_3H. In presence of water the proton resides exclusively in the aqueous portion of the solvent mixture and the acid dissociation becomes complete.[16] One may tune the size of the protonated water solvates formed by acid dissociation by controlling the water-to-acid molar ratio in acetonitrile. Most importantly, by use of acetonitrile, we can maintain a large population of $H_5O_2^+$ in a local minimum formed by the solvent cage, with exchange between different hydrated proton solvates occurring on time scales much longer than those dictating the vibrational transition line shapes. With this approach we circumvent the complicating matter of potentially different hydrated proton species due to proton transport and ultrafast fluctuations in the structure of the extended hydrogen-bond network in aqueous solution. Using "Zundel cation" as a dedication to Georg Zundel's pioneering work,[8,14] we understand that $H_5O_2^+$ in acetonitrile will not be strictly symmetric at all times, but has a fluxional degree in its structure.[17]

For our purposes, $H_5O_2^+$ is formed by hydrating the H^+ from the fully dissociated $HClO_4$ with two water molecules while the ClO_4^- counter anion is completely separated from the proton and fully solvated by acetonitrile (Figure 1a). The remaining water exists mainly in form of monomers while the concentration of H_3O^+ is less than 10% of $H_5O_2^+$ (see the Supporting Information). In Figure 1b, the linear absorption spectrum of $H_5O_2^+$ (red line) is shown, after subtraction of the solvent background (gray line). Infrared-active marker transitions of $H_5O_2^+$ are the OH bending absorption at 1740 cm^{-1}, the OH stretching band at 3400 cm^{-1}, and the so-called

[*] F. Dahms, Dr. R. Costard, Dr. B. P. Fingerhut, Dr. E. T. J. Nibbering, Prof. Dr. T. Elsaesser
Max Born Institut für Nichtlineare Optik und Kurzzeitspektroskopie
Max Born Strasse 2A, 12489 Berlin (Germany)
E-mail: nibberin@mbi-berlin.de
elsasser@mbi-berlin.de
Prof. Dr. E. Pines
Department of Chemistry, Ben Gurion University of the Negev
P.O.B. 653, Beersheva 84105 (Israel)

Supporting information for this article can be found under: http://dx.doi.org/10.1002/anie.201602523.

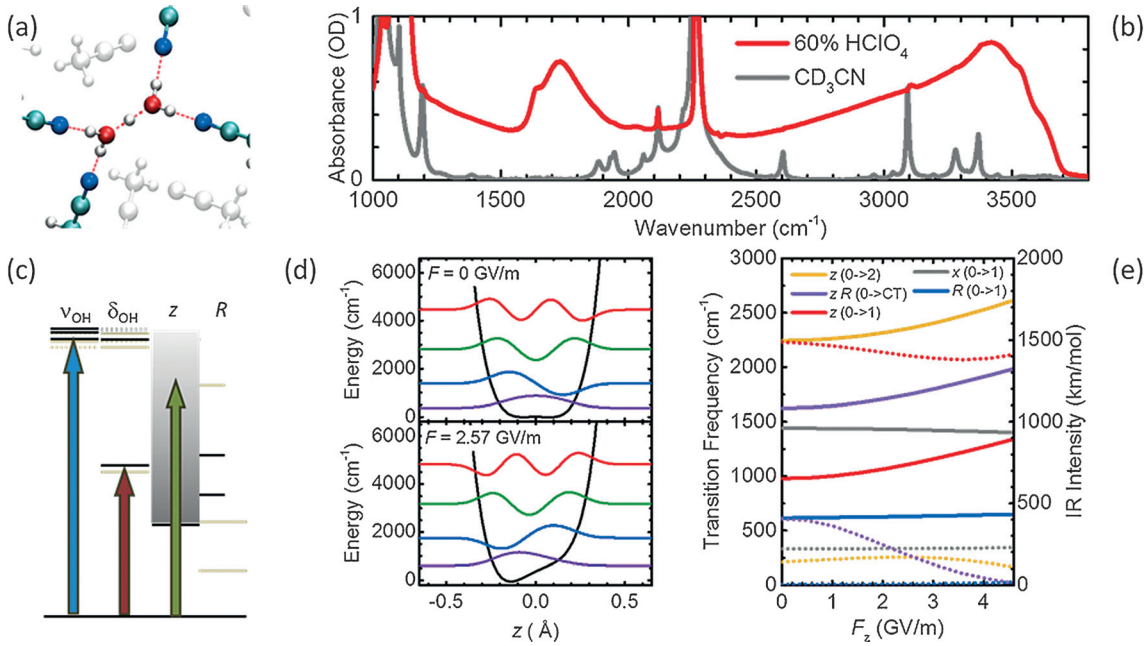

Figure 1. a) Schematic of the Zundel cation $H_5O_2^+$ in acetonitrile solution. b) Linear infrared spectrum of $H_5O_2^+$ solution (red line) minus the absorption of acetonitrile (gray line). c) Level scheme of $H_5O_2^+$vibrations (OH stretching (ν_{OH}), OH bending (δ_{OH}), proton transfer mode *z*, and O···O mode *R*); black indicates states of IR-active modes, gray of Raman-active modes. The length of arrows is scaled according to the experimental excitation frequencies used in this study. d) Calculated vibrational potential and wavefunctions of the lowest vibrational states of *z* for $R = 2.45$ Å for external fields $F_z = 0$ and $F_z = 2.57$ GV m^{-1}. e) Calculated transition frequencies (solid lines) and absorption strengths (dotted lines) as a function of the external field F_z, calculated for the *z*, *R* and *x* fundamental, and *z* first overtone transition, as well as the combination tone of *z* with *R*; *x* is the proton out-of-plane coordinate orthogonal to *z* with a transition frequency weakly affected by F_z. A field amplitude of 1 GV m^{-1} = 10^9 V m^{-1} corresponds to 10 MV cm^{-1} or 0.1 V Å^{-1}.

Zundel continuum[18] between 1000 and about 3000 cm^{-1} (schematic level diagram in Figure 1c).

Transient vibrational spectra were measured with femtosecond pump pulses centred at 3400 cm^{-1} in the OH stretching band and at 2700 cm^{-1} in the absorption continuum (dotted lines in Figure 2a). In Figure 2b,c, the change of absorbance $\Delta A = -\log_{10}(T/T_0)$ is plotted as a function of probe frequency for different pump-probe delays (T, T_0: sample transmission with and without excitation). After excitation at 3400 cm^{-1} (Figure 2b), the spectra display an absorbance decrease for frequencies above 3250 cm^{-1}, due to ground state bleaching on the $v = 0$ to 1 and stimulated emission on the $v = 1$ to 0 transition of the OH stretching oscillator of $H_5O_2^+$. The absorption increase below 3250 cm^{-1} is caused by the OH stretching $v = 1$ to 2 absorption. The enhanced absorption at 3130 cm^{-1} (Figure 3a, black arrow in Figure 2b) and, thus, the $v = 1$ population decays within the time resolution of the experiment, setting an upper limit of 50 fs for the $v = 1$ lifetime, followed by slow kinetics extending into the picosecond regime (cf. the Supporting Information). The fast decay time is two orders of magnitude shorter than in water monomers[19] and a factor of four shorter than in bulk H_2O.[20] Transients recorded at 3435 cm^{-1} (Figure 3a, red arrow in Figure 2b) characterizing the bleaching component in the spectra of Figure 2b show similar kinetics, with the slow component much more pronounced (cf. the Supporting Information). This signal is attributed to a hot ground state of $H_5O_2^+$ generated by the redistribution of excess energy. Its decay with a 2.7 ps time constant (solid line in Figure 3a; cf. the Supporting Information) is due to the transfer of excess energy to the solvent.

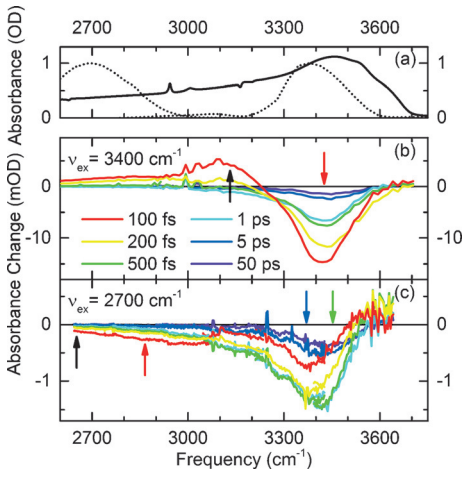

Figure 2. a) Linear infrared absorption spectrum (solid line) and spectra of the pump pulses (dotted lines). b,c) Transient infrared absorption spectra for pump-probe delays between 100 fs and 50 ps. The absorbance change ΔA is plotted as a function of probe frequency. The spectra in (b) and (c) were recorded with excitation centered at 3400 and 2700 cm^{-1}, respectively.

The transient spectra measured with excitation at 2700 cm^{-1} (Figure 2c) consist of a spectrally broad absorption decrease up to 3500 cm^{-1}, that is, well above the excitation pulse, while an absorption increase occurs above 3500 cm^{-1}.

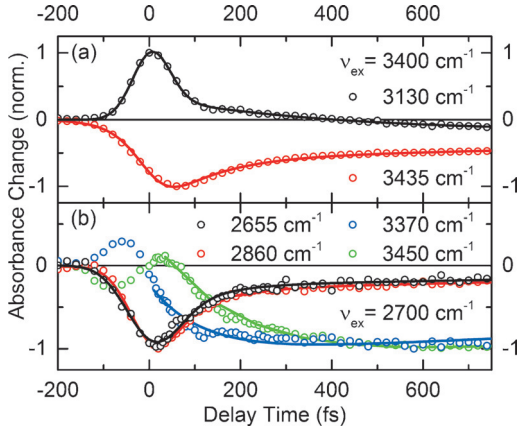

Figure 3. Time-resolved absorbance changes for excitation centred at a) 3400 cm^{-1} and b) 2700 cm^{-1}. The normalized absorbance changes at fixed probe frequencies (circles) are plotted as a function of pump-probe delay. Time constants derived from numerical fits (solid lines) are given in the Supporting Information.

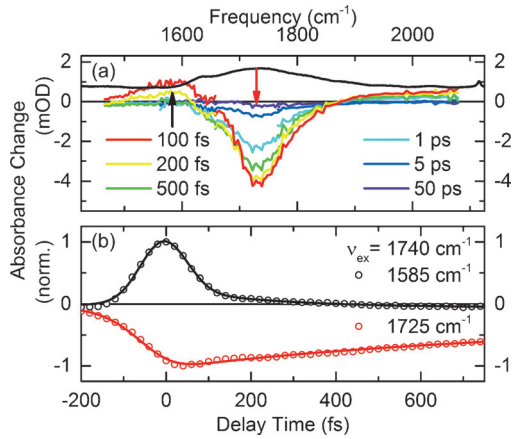

Figure 4. a) Transient OH bending spectra and b) time-resolved absorbance change after excitation with pump pulses centered at 1740 cm^{-1}. The solid line in (a) represents the linear infrared absorption spectrum. Time constants derived from numerical fits (solid lines) are given in the Supporting Information.

Different contributions are distinguished via their markedly different time evolution. Figure 3b displays transients measured at the frequency positions marked by arrow in Figure 2c. Below 3250 cm^{-1}, we observe a quasi-instantaneous increase of the bleaching signal, followed by a pronounced fast decay with a time constant shorter than 65 fs and a weaker long-lived component reflecting vibrational heating. In contrast, the onset of bleaching above 3250 cm^{-1} becomes increasingly delayed and ends up in the long-lived heating signal. The absorption decrease below 3250 cm^{-1} is due to vibrational excitations distinctly different from the OH stretching mode of $H_5O_2^+$ which is not excited by the pump pulses at 2700 cm^{-1}. The absorption changes above 3250 cm^{-1} are a hallmark of the vibrationally hot ground state of $H_5O_2^+$ in which low-frequency modes of the cation are strongly populated. Anharmonic coupling of low-frequency excitations to the OH stretching mode result in a blue-shifted $v=0$ to 1 transition of the latter as is evident from the bleaching between 3250 and 3500 cm^{-1} and the enhanced absorption above 3500 cm^{-1}. The measured rise times depend on the particular probe frequency (Figure 3b), reflecting the sub-picosecond formation of the hot ground state.

In an independent series of measurements, we investigated the OH bending mode of $H_5O_2^+$. After resonant excitation of the $v=0$ to 1 transition by pulses centered at 1740 cm^{-1}, the transient spectra in Figure 4a exhibit the enhanced $v=1$ to 2 absorption and the bleaching on the $v=0$ to 1 transition. The enhanced absorption decays with a time constant shorter than 60 fs (Figure 4b). This upper limit of the $v=1$ lifetime is shorter than the 170 fs lifetime of the OH bending mode in neat H_2O. The $v=0$ to 1 bleaching shows a slower time evolution due to strong thermal signals which contribute at long delay times and are present also at probe frequencies above the pulse spectrum, for example, at 1900 cm^{-1} in the Zundel continuum.

As a key finding, our data demonstrate the spectrally and kinetically distinct response of the OH bending mode, the H^+ infrared absorption continuum, and the OH stretching mode. In particular, the so-called Zundel continuum below and the OH stretching absorption above approximately 3000 cm^{-1} represent different types of vibrational excitations. Occurrence and origin of the infrared continuum have remained highly controversial in the existing literature, dating back to the work of Zundel.[8] Originally a large proton polarizability has been understood to result from the interplay of a double-well potential for the proton transfer coordinate z,[14] due to a strong hydrogen bond (sometimes called a "special bond"), and large electrical fields imposed by the surrounding medium. An inhomogeneous distribution of electrical fields has been invoked to explain why the large proton polarizability results in broad IR absorption continua.[14b]

We now present theoretical results which are based on the formalism described in the Supporting Information and elucidate the key role of the so-called proton transfer mode z in the O···H$^+$···O moiety for the absorption continuum. Figure 1d shows the calculated potential along the O···H$^+$···O coordinate of the isolated system, along with the wavefunctions of the vibrational quantum states. The height of the central barrier depends critically on the O···O distance R and is found to remain below the ground state vibrational level for R < 2.60 Å as is discussed in the Supporting Information.[14] The polar acetonitrile environment generates a strong electrical field with a component on the order of $F_z = 3\times10^9$ V m^{-1} ($=3$ GV m$^{-1}=30$ MV cm^{-1})[21] along the vibrational coordinate z. For such fields the vibrational potential of the bare $H_2O_5^+$ is significantly distorted which results in a shift of vibrational levels and transition frequencies (Figure 1d). The calculated frequencies of different vibrational transitions are plotted as a function of the electrical field amplitude in Figure 1e, along with their absorption strengths. For isolated $H_5O_2^+$ in the gas phase it is commonly established that the barrier in the double minimum potential clearly lies much lower in energy than the $v=0$ state for the z coordinate.[7b] Based on our calculations we conclude that this picture remains valid for $H_5O_2^+$ subject to electrical fields typical for acetonitrile. Hence, proton localization on one

water molecule, producing a long-lived species $H_3O^+\cdots OH_2$, can only be accomplished when the two oxygen atoms are separated by more than $R = 2.60$ Å. This O···O separation is larger than the equilibrium distance of R in $H_5O_2^+$ reported on the order of 2.40–2.55 Å.[1,8] We emphasize here that the impact of these electrical fields on the resulting vibrational spectra is much larger than those characterized for the cases of noble gas atom tagged $H_5O_2^+$ in the gas phase.[22] In frozen hydrated proton clusters where different proton geometries are distinguished due to the absence of structure fluctuations, a strong impact of electric fields on the potential energy surface has been found as well.[18b]

We ascribe the origin of the markedly larger Zundel continuum observed for $H_5O_2^+$ in solution to the fact, that at ambient temperature, the spatial arrangement of solvent molecules undergoes rapid fluctuations on a multitude of time scales with the fastest components in the sub-100 fs domain.[23] Such structure fluctuations translate into fluctuating electrical fields and, consequently, a fluctuating vibrational potential of the Zundel cation. The latter is connected with strong frequency excursion of different vibrational transitions (cf. Figure 1e), in particular of the $v = 0$ to 1 transition of the proton transfer mode, while changes of the transition dipole moments are limited (less than 30%). In this way, an absorption continuum covering several 100 cm^{-1} is generated. In addition to the $v = 0$ to 1 transition, the $v = 0$ to 2 overtone transition of the proton stretching vibration z as well as combination tones with the O···O stretching vibration R fundamental at 580 cm^{-1} have appreciable transition dipole moments (Figure 1e), making all contribute to the absorption continuum. A second source of fluctuating transition frequencies and, thus, broadening, are stochastic thermal excitations of the O···O mode. This effect will be particularly pronounced in the hot ground state which is generated by energy dissipation and characterized by vibrational temperatures up to $T = 1000$ K ($kT = 670$ cm^{-1}). In the $v = 1$ state of the O···O mode, the O···O distance changes by approximately 0.1 Å, resulting in an appreciable change of the vibrational potential and a concomitant shift of transition frequencies.

We consider such two mechanisms the origin of the extreme broadening of the infrared absorption continuum. Instead of having a distribution of different cation geometries, that is, an inhomogeneous distribution of vibrational transition frequencies such as in gas-phase clusters,[18b] the ultrafast solvent-induced modulation of the proton transfer mode potential causes the infrared absorption continuum in solution. As shown by the pump-probe data the continuum efficiently funnels vibrational excess energy of the OH bending and stretching transitions into low frequency modes of the Zundel cation.

Fluctuating electrical fields with even larger amplitudes occur in neat water and, thus, long-range structural fluctuations of water must have a fundamental impact on structure and dynamics of the hydrated proton in bulk water in addition to short-range fluctuations in the hydrogen-bonding network of the water molecules. This intriguing aspect of ultrafast solvent-induced proton potential modulation should be taken into account, together with the extremely short vibrational lifetimes, in the interpretation of ultrafast IR pump-probe and multidimensional IR photon echo studies of aqueous proton solutions.[12,13] It also sets limits for the persistence of any distinctive proton solvation patterns in bulk water. Ultimately a sophistication of the understanding of structural dynamics of hydrated protons in water appears to be the goal in future studies.

Acknowledgements

B.P.F. gratefully acknowledges support through the DFG within the Emmy Noether Programme (grant number FI 2034/1-1)

Keywords: femtochemistry · hydrated protons · solvation dynamics · Zundel cation · Zundel continuum

How to cite: *Angew. Chem. Int. Ed.* **2016**, *55*, 10600–10605
Angew. Chem. **2016**, *128*, 10758–10763

[1] D. Marx, M. E. Tuckerman, J. Hutter, M. Parrinello, *Nature* **1999**, *397*, 601–604.
[2] K. D. Kreuer, S. J. Paddison, E. Spohr, M. Schuster, *Chem. Rev.* **2004**, *104*, 4637–4678.
[3] O. F. Mohammed, D. Pines, J. Dreyer, E. Pines, E. T. J. Nibbering, *Science* **2005**, *310*, 83–86.
[4] E. Freier, S. Wolf, K. Gerwert, *Proc. Natl. Acad. Sci. USA* **2011**, *108*, 11435–11439.
[5] a) K. R. Asmis, N. L. Pivonka, G. Santambrogio, M. Brümmer, C. Kaposta, D. M. Neumark, L. Wöste, *Science* **2003**, *299*, 1375–1377; b) T. D. Fridgen, T. B. McMahon, L. MacAleese, J. Lemaire, P. Maitre, *J. Phys. Chem. A* **2004**, *108*, 9008–9010; c) J. M. Headrick, E. G. Diken, R. S. Walters, N. I. Hammer, R. A. Christie, J. Cui, E. M. Myshakin, M. A. Duncan, M. A. Johnson, K. D. Jordan, *Science* **2005**, *308*, 1765–1769.
[6] G. Zundel, H. Metzger, *Z. Phys. Chem.* **1968**, *58*, 225–245.
[7] a) X. Huang, B. J. Braams, J. M. Bowman, *J. Chem. Phys.* **2005**, *122*, 044308; b) O. Vendrell, F. Gatti, H.-D. Meyer, *J. Chem. Phys.* **2007**, *127*, 184303.
[8] H.-H. Limbach, P. M. Tolstoy, N. Pérez-Hernández, J. Guo, I. G. Shenderovich, G. Denisov, *Isr. J. Chem.* **2009**, *49*, 199–216.
[9] E. Wicke, M. Eigen, T. Ackermann, *Z. Phys. Chem.* **1954**, *1*, 340–364.
[10] a) N. Agmon, *Chem. Phys. Lett.* **1995**, *244*, 456–462; b) R. Vuilleumier, D. Borgis, *J. Chem. Phys.* **1999**, *111*, 4251–4266; c) D. Marx, *ChemPhysChem* **2006**, *7*, 1848–1870; d) A. Hassanali, F. Giberti, J. Cuny, M. Parrinello, *Proc. Natl. Acad. Sci. USA* **2013**, *110*, 13723–13728; e) J. Xu, Y. Zhang, G. A. Voth, *J. Phys. Chem. Lett.* **2011**, *2*, 81–86; f) W. Kulig, N. Agmon, *Nat. Chem.* **2013**, *5*, 29–35.
[11] A. Botti, F. Bruni, M. A. Ricci, A. Soper, *J. Chem. Phys.* **2006**, *125*, 014508.
[12] S. Woutersen, H. J. Bakker, *Phys. Rev. Lett.* **2006**, *96*, 138305.
[13] M. Thämer, L. De Marco, K. Ramasesha, A. Mandal, A. Tokmakoff, *Science* **2015**, *350*, 78–82.
[14] a) R. Janoschek, E. G. Weidemann, H. Pfeiffer, G. Zundel, *J. Am. Chem. Soc.* **1972**, *94*, 2387–2396; b) G. Zundel, *Adv. Chem. Phys.* **2000**, *111*, 1–217.
[15] N. Ben-Menachem Kalish, E. Shandalov, V. Kharlanov, D. Pines, E. Pines, *J. Phys. Chem. A* **2011**, *115*, 4063–4075.
[16] a) I. M. Kolthoff, M. K. Chantooni, Jr., *J. Am. Chem. Soc.* **1968**, *90*, 3320–3326; b) M. K. Chantooni, Jr., I. M. Kolthoff, *J. Am. Chem. Soc.* **1970**, *92*, 2236–2239.
[17] a) M. Baer, D. Marx, G. Mathias, *Angew. Chem. Int. Ed.* **2010**, *49*, 7346–7349; *Angew. Chem.* **2010**, *122*, 7504–7507; b) A. A.

Hassanali, J. Cuny, M. Ceriotti, C. J. Pickard, M. Parrinello, *J. Am. Chem. Soc.* **2012**, *134*, 8557 – 8569.
[18] a) P. Ayotte, M. Hébert, P. Marchand, *J. Chem. Phys.* **2005**, *123*, 184501; b) J. A. Fournier, C. T. Wolke, M. A. Johnson, T. T. Odbadrakh, K. D. Jordan, S. M. Kathmann, S. S. Xantheas, *J. Phys. Chem. A* **2015**, *119*, 9425 – 9440.
[19] D. Cringus, T. l. C. Jansen, M. S. Pshenichnikov, D. A. Wiersma, *J. Chem. Phys.* **2007**, *127*, 084507.
[20] M. L. Cowan, B. D. Bruner, N. Huse, J. R. Dwyer, B. Chugh, E. T. J. Nibbering, T. Elsaesser, R. J. D. Miller, *Nature* **2005**, *434*, 199 – 202.
[21] S. D. Fried, S. G. Boxer, *Acc. Chem. Res.* **2015**, *48*, 998 – 1006.
[22] a) N. I. Hammer, E. G. Diken, J. R. Roscioli, M. A. Johnson, E. M. Myshakin, K. D. Jordan, A. B. McCoy, X. Huang, J. M. Bowman, S. Carter, *J. Chem. Phys.* **2005**, *122*, 244301; b) T. C. Cheng, B. Bandyopadhay, J. D. Mosley, M. A. Duncan, *J. Am. Chem. Soc.* **2012**, *134*, 13046 – 13055; c) C. J. Johnson, A. B. Wolk, J. A. Fournier, E. N. Sullivan, G. H. Weddle, M. A. Johnson, *J. Chem. Phys.* **2014**, *140*, 221101.
[23] D. McMorrow, W. T. Lotshaw, *J. Phys. Chem.* **1991**, *95*, 10395 – 10406.

Received: March 11, 2016
Published online: July 4, 2016

